主論文

Development of the extracellular structure is crucial for acquisition of sound sensitivity by inner ear hair cells

(細胞外構造の発達が内耳有毛細胞の音受容能獲得に重要である)

Maya Inoue

井上　摩耶

Division of Biological Science

Graduate School of Science

Nagoya University

Table of Contents

1. Abstract

Hearing and body balance are perceived as different senses; however, they are initiated by a common system of mechanotransduction through inner ear hair cells. Sound- or head movement-evoked mechanical displacement is converted into electrical signals by opening the mechanotransduction channels located at the tips of inner ear hair cells. In addition to the mechanotransduction machinery, extracellular structures surrounding hair cells are essential for detecting tiny movements evoked by sound and head motion. In particular, hearing sensitivity is remarkably high enough to respond to sub-nanometer air vibrations. However, the precise function of the extracellular structures in sound detection has been difficult to determine *in vivo* because of their delicate structures and inaccessible location in the deeper part of the head. In this study, I used embryonic and larval zebrafish and conducted an *in vivo* examination of the roles of the extracellular structures on hearing by eliminating or manipulating the size of the ear stone, or otolith, which is an extracellular biomineral structure, in sensory receptor organs (saccule and utricle). Microphonic potentials, which reflect hair cell mechanotransduction, revealed that fish received sound in the saccule, not in the utricle. Observations of developmental changes in otolith organs showed that the otolith in the saccular macula grew markedly and became considerably larger than that in the utricle, and that this was concurrent with the acquisition of sound sensitivity. When the utricular otolith was experimentally enlarged, utricular hair cells exhibited acoustic responses, indicating that the otolith

size was a key in sound detection. When otoliths, particularly saccular otoliths were removed from the maculae, they did not grow as large as those that were intact, suggesting that otolith biomineralization occurs in a region-specific manner. These *in vivo* analyses clarified an important aspect of the relationship between sound responsiveness of hair cells and associated extracellular structures in the acquisition of hearing.

2. Introduction

2.1 Detection of sensory signals in animals

Animals use various senses to identify the surrounding activities. Vision, smell, taste, touch, and hearing are the traditionally recognized sensations. These sensory modalities are mediated by distinct types of receptor cells located in the specific sensory organs. The classic five senses and sense of body balance are mediated by receptors in the eye, nose, mouth, skin, and inner ear. The other somatosensory modalities, including temperature, pain, and proprioception, are mediated by receptors distributed throughout the body. The principal receptor cells are photoreceptors (vision), chemoreceptors (smell, taste, and pain), thermal receptors (temperature), and mechanoreceptors (touch, hearing, balance, and proprioception).

The sensitivities of sensory receptor cells are remarkably high. For instance, a rod photoreceptor in the eye is sensitive enough to respond to a single photon of light (**Baylor et al., 1979**). Meissner's corpuscle, distributed in various areas of the skin, can detect bumps smaller than 10 μm (**Johansson, 1978**). Thermal sensory neurons are sensitive enough to detect a temperature difference of approximately 0.1°C (**Kenshalo et al., 1960**). Auditory hair cells in the inner ear are activated at a 0 dB sound pressure level (SPL re 20 μPa) by air molecule displacement of only 10 pm (10^{-11} m) (**Wheeler and Dickson, 1952**).

Specialized structures with specific receptors and related molecules are essential for achieving

the high sensitivities of receptor cells. Further, the extracellular structures surrounding receptor cells are essential for capturing the sensory stimuli and effectively transmitting them to the receptor cells.

2.2 Auditory and vestibular sensory organs in mammals

Hearing and balance are different senses; however, sensory stimuli for both senses are detected by sensory hair cells in the ear (described in the next section). The inner ear structure within the petrous portion of the temporal bone is divided into several parts for auditory and vestibular signal detection, and each part contains hair cells. In the mammalian inner ear, the cochlea transduces sound stimuli, whereas otolith organs and semicircular canals transduce linear and angular acceleration, respectively (**Fig.1a**). The cochlea is a coiled bony tube. Furthermore, the auditory sensory organ, or the organ of Corti, is located within the cochlear duct, and it is on the flexible basilar membrane. Basilar membrane vibrations create a shearing force against the stationary tectorial membrane, causing hair bundle deflection in that plane. Two otolith organs (saccule and utricle) contain a sensory macula, comprising hair cells and supporting cells situated beneath calcium carbonate crystals (otoconia or otoliths) that are embedded in a gelatinous mass (otolithic membrane). When the head undergoes linear acceleration, the greater relative mass of the otolithic membrane causes it to temporarily lag behind the macula, resulting in a transient displacement of hair bundles. The semicircular canals are three orthogonal (at 90°) bony structures, wherein the hair cells sense the

endolymph movement that occurs during rotational acceleration.

Although the auditory and vestibular organs have specialized structures, both house sensory hair cells for detecting sensory signals. What is the essential difference between auditory and vestibular organs? In this study, I used zebrafish larvae, which possess primitive auditory organs structurally similar to the vestibular one (described in section 2.6), to clarify the mechanisms underlying the functional differentiation between auditory and vestibular sensory organs.

2.3 Mechanotransduction in inner ear hair cells

The first step in receiving acoustic or vestibular stimuli is deflection of hair bundles on the apex of the hair cell that causes hair cell depolarization by ion influx through the mechanically gated channels (mechanotransduction, **Fig. 2**, **Hudspeth, 1989**).

Hair bundles comprise numerous cylindrical processes, or the stereocilia, comprising a fascicle of actin filaments and single microtubule-based cilium, or the kinocilium. The stereocilia are organized into bundles with a characteristic staircase-like pattern. The kinocilium sits next to the tallest edge of the stereocilia, although it retracts and disappears postnatally in hair cells in auditory organs of mammals and birds. The tip of the shorter stereocilium is connected to the side of the adjacent longer cilium by a tip link. The tip link acts as the gating string: a stimulus toward the tall edge of hair bundles increases tension in the tip link, and opens a mechanotransduction channel on

the stereocilium tip (**Beurg et al., 2009**). Further, the upper two-thirds of the tip link comprise a parallel homodimer of cadherin 23 molecules, and the lower third contains a parallel homodimer of protocadherin 15 chains (**Kazmierczak et al., 2007**; **Lelli et al., 2010**). These mechanisms and components of hair cells are common to both auditory and vestibular hair cells.

2.4 Developmental acquisition of mechanotransduction in hair cells

How do animals obtain the senses of sound and balance during development? The first step is to acquire mechanotransduction in inner ear hair cells. In the mouse utricle, hair bundles first appear on the embryonic day (E) 13.5 (**Denman-Johnson and Forge, 1999**), and the tip links mutually connecting stereociliary bundles appear between E15 and E17 (**Geleoc and Holt, 2003**). Concomitantly, hair cells exhibit mechanotransduction channels and mechanotransducer currents through the channels between E16 and E17 (**Geleoc and Holt, 2003**). The developmental sequence of cochlear hair cells is same as above in chick and mouse (**Si et al., 2003**; **Waguespack et al., 2007**; **Lelli et al., 2009**). These findings were obtained in studies that used isolated hair cells or dissected maculae. However, it remained unclarified when and how hair cells begin to operate *in vivo* in vertebrates.

In a previous study, we performed an *in vivo* study of the developmental acquisition of mechanosensitivity in macular hair cells in zebrafish embryo (**Tanimoto et al., 2011**). Zebrafish,

Danio rerio, is a widely studied vertebrate for the function of the inner ear. The transparency of zebrafish embryos and larvae enables the direct observation of the formation of the inner ear and development of hair cells (**Haddon and Lewis, 1996**; **Riley et al., 1997**; **Whitfield et al., 2002**; **Abbas et al., 2010**). In early embryonic zebrafish, over a hundred ciliary cells appear in the otic vesicle (OV) around 19 h post-fertilization (hpf) (**Riley et al., 1997**; **Stooke-Vaughan et al., 2012**). Most ciliary cells gradually decrease their ciliary length by 24 hpf and subsequently lose their cilia. On the other hand, two or three ciliary cells at the anterior and posterior OV poles each elongate their cilia and attach the otolith to their tips by 20 hpf (**Riley et al., 1997**). These cells are called tether cells. Moreover, the motility of cilia that are present near the tether cells is necessary for the formation and positioning of otoliths (**Riley et al., 1997**; **Wu et al., 2011**; **Stooke-Vaughan et al., 2012**). Otolith precursor particles that are initially distributed throughout OV are gradually tethered to the tips of tether cilia depending on the flow forces generated by beating cilia, and they form two otoliths at the anterior and posterior poles. Tether cells are believed to be precursory form of hair cells because of their location, number, and tubulin-immunoreactive pattern in the cell body (**Riley et al., 1997**). However, thus far, the appearance of stereocilia, mechanotransduction channels, tip links, and the electrophysiological properties of tether cells had not been elucidated. By investigating the morphological and functional development of tether cells, we demonstrated that tether cells acquire mechanosensitivity and become the first hair cell in the inner ear (**Tanimoto et al., 2011**).

The stereocilia appeared on the apex of tether cell at 22 hpf, and they increased in ciliary length to more than 24 hpf. Mechanotransduction concurrently occurred with the appearance of the mechanotransduction channels in tether cells at 23 hpf. Another study has indicated that the tip links, which are necessary for mechanotransduction of hair cells, appear on tether cells by 24 hpf (**Sollner et al., 2004**; **Seiler et al., 2005**). Together, these results indicated that only within an hour after the stereocilia begin to extend their length, the mechanotransduction components are assembled and become functional in zebrafish (**Fig. 3**).

To summarize, mechanotransduction is acquired by the following sequence in fish, chick and rodent hair cells. First, hair bundles appear on the apex of the hair cell. Further, the components of the mechanotransduction machinery, tip links and mechanotransduction channels, are assembled. Simultaneously, the machinery begins to function.

2.5 Hearing onset and developmental changes of extracellular structures

Auditory responsiveness of hair cells is obtained later than the acquisition of mechanosensitivity, probably because the receptor organ requires development of other components to acquire enough sensitivity to detect sound-evoked vibration. In rat and mouse, sound-evoked responses in a auditory-recipient neurons in the brainstem appear at postnatal day 11–12 (P11–12), which is much later than the start of hair cell mechanotransduction and formation of the functional auditory afferent pathway (P1) (**Blatchley et al., 1987**; **Geal-Dor et al., 1993**; **Waguespack et al., 2007**; **Lelli et al.,**

2009; Lenoir et al., 1980; Sobkowicz et al., 1982; Neises et al., 1982; Limb and Ryugo, 2000). Similarly, there is a delay (20 h) from the acquisition of mechanotransduction in zebrafish hair cells to the appearance of auditory responses in brainstem neurons, such as hindbrain Mauthner cells which are known to initiate sound-evoked fast escape behavior in fish (Tanimoto et al., 2009, 2011). The coincident acquisition of auditory responsiveness of hair cells and Mauthner cells indicates that hair cell responsivity to sound is critical for auditory perception in the brainstem (Tanimoto et al., 2009). However, the key mechanism in the acquisition of sound responsiveness in hair cells after the onset of mechanotransduction remains unelucidated.

Morphological observations in rodents suggest that development of cochlear structures is necessary for sound detection in hair cells. The growth of the tectorial membrane for covering hair cells is coincident with the onset of hearing in rodents (Roth and Bruns, 1992; Rueda et al., 1996; Kopecky et al., 2012). The tectorial membrane plays a crucial role in the transmission of basilar membrane motion to the sensory hair bundles. However, because of its inaccessible location and susceptibility to changes in its unique ionic environment in the organ of Corti, the precise function of the tectorial membrane in hearing has been hard to determine in mammals. For *in vivo* studies of the auditory system, minimally invasive measures, such as, compound action potentials of the auditory nerve, are used. However, there are many aspects of cochlear physiology that cannot be unambiguously inferred from these gross responses. Cochlea microphonic potential (extracellular

receptor potential), which reflects hair cell mechanotransduction responses, can be recorded in rodents *in vivo* (**Legan et al., 2005**; **Russell et al., 2007**). However, recording is limited in the basal turn of the cochlea because of the inaccessibility to the apical part.

Therefore, zebrafish are very useful in the investigation of hair cell responsiveness and contribution of extracellular structures to sound sensitivity *in vivo*. Because zebrafish embryos and larvae are transparent and have a simple inner ear organ, the structure can be observed and hair cell responses can be directly recorded (**Fig. 5**). Furthermore, because fish use simple auditory organs (described in section 2.6), the extracellular structure covering the hair cells can be manipulated and its role in sound detection can be investigated by recording sound-evoked responses from whole hair cells in the ear.

2.6 Auditory and vestibular signal sensing in zebrafish

The adult fish ear comprises three orthogonally arranged semicircular canals and three otolith organs (**Fig. 1b**; **Abbas et al., 2010**). The cochlea is absent in fish; they receive linear acceleration and sound input in otolith organs (utricle, saccule, and lagena) (**von Frisch, 1938**; **Popper and Fay, 1993, 2011**). The otolith organs contain macular sensory hair cells coupled with an otolith, a biomineralized ear stone composed of calcium carbonate and proteins. The otolith acts as an inertial mass, and sound- and head movement-evoked acceleration produces relative displacement between

the otolith and the coupled hair cells because of differences in their inertia (**Fig. 4**). This displacement mechanically deflects the hair bundles and opens mechanotransduction channels, which subsequently produces a receptor potential (**Popper and Fay, 1993, 2011**). A behavioral study, involving selective elimination of the otolith organ in adult fish, has revealed the functional differences between the three otolith organs: the saccule (S) and lagena (L) are necessary for auditory perception, and the utricle (U) is essential for postural equilibrium (**von Frisch, 1938**). However, the mechanisms underlying their functional differentiation remain unclear.

In larval zebrafish, before 15 days post-fertilization (dpf), the main components of the ear are five sensory patches of sensory epithelium; two maculae of otolith organs and three cristae of semicircular canals. The two maculae, S and U, are the first sensory patches, and they appear by 1 dpf at the posterior and anterior OV poles, respectively (described in section 2.4). The hair cells of L start to differentiate at 15 dpf (**Bever and Fekete, 2002**). The three canals and their sensory patches are formed by 3 dpf, but they do not become functional until after 30 dpf (**Beck et al., 2004**). Although zebrafish larvae at 5 dpf have only two functional sensory organs, the U and S otolith organs, in the ear, it is clear from behavioral observations that they definitely sense sound and maintain body posture (**Riley and Moorman, 2000**; **Kimmel et al., 1974**; **Zeddies and Fay, 2005**). The contribution of U, not S, to vestibular behavior (body posture and vestibulo-ocular reflex) has been demonstrated (**Riley and Moorman, 2000**; **Bianco et al., 2012**). However, whether the sound

stimuli are detected by U and/or S has not been examined by *in vivo* recordings from hair cells. It also remains unclear how these otolith organs receive each modality separately, despite the similarity of their structures, composed of an otolith and hair cells.

2.7 Overview

In this study, I aim to determine the key process in the acquisition of sound sensitivity by hair cells and how sound is distinguished from vestibular stimuli. I compared sound responsiveness of the structurally similar U and S otolith organs and observed the developmental changes of otoliths in each macula for investigating the contribution of the extracellular structure to the acquisition of sound sensitivity in hair cells. In addition, I examined effects of otolith manipulation on the sound sensitivity of hair cells.

First, in order to examine whether U or S was associated with sound detection in larvae, I recorded sound-evoked microphonic potentials (MPs), which reflect hair cell mechanotransduction responses in OVs. Further, to eliminate the function of either U or S otolith organ, I removed one of the two otoliths at 2 dpf and recorded the hair cell responses at 5 dpf when fish acquire hearing and bodily balance (**Riley and Moorman, 2000**; **Kimmel et al., 1974**; **Zeddies and Fay, 2005**). In larvae, sound was predominantly received by the S hair cells and not by the U hair cells.

Second, I observed developmental changes in otolith organs and showed the day-by-day otolith growth in each otolith organ. At first, the otolith sizes were almost the same between the two; however, the S otolith markedly increased in size and grew much larger than the U otolith on and after 2 dpf. The otolith size appeared to be an important factor in differentiating the sound sensitivity of the U and S otolith organs because a large otolith was believed to be suitable for the detection of sound (see Results). Furthermore, the time when the otolith size appeared to differ between S and U was concurrent with the acquisition of sound sensitivity (**Tanimoto et al., 2009**).

I established an *in vivo* method for the micromanipulation of otolith size for investigating the effects of the difference in the otolith size on sound sensitivity, and demonstrated that enlarged otoliths enabled U hair cells to exhibit acoustic responses. These results suggested that macular region-dependent otolith formation and regulation of the extracellular structure size were crucial for effectively and separately receiving auditory information. To the best of our knowledge, this is the first direct demonstration to show the role of the extracellular structure in hair cell sound sensitivity *in vivo*.

a

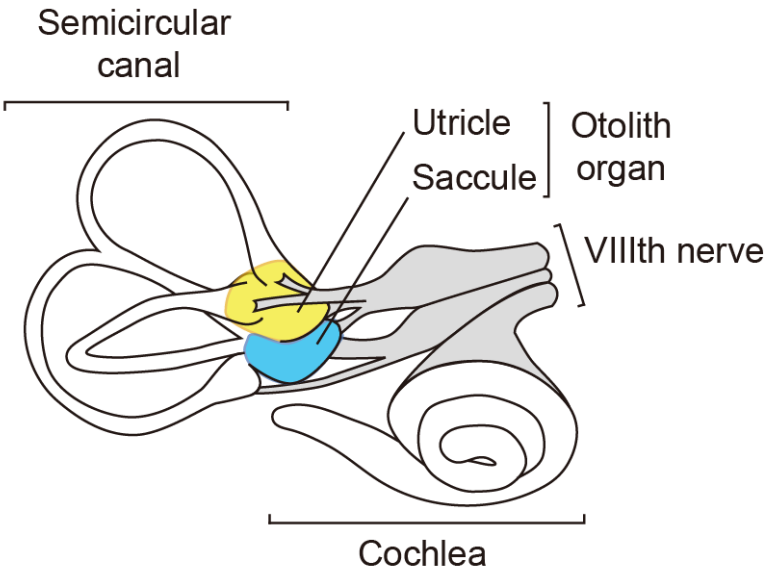
Semicircular canal
Utricle
Saccule
Otolith organ
VIIIth nerve
Cochlea

b

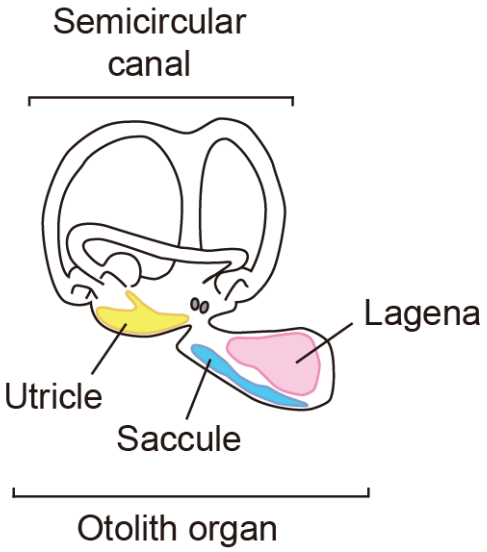
Semicircular canal
Lagena
Utricle
Saccule
Otolith organ

Fig. 1

Fig. 1 Inner ear structures in mammal and fish

(**a**) The mammalian inner ear comprises of the cochlea, otolith organs (utricle and saccule), and semicircular canals. The cochlea transduces sound stimuli, whereas otolith organs and semicircular canals transduce linear and angular acceleration, respectively. (**b**) The fish inner ear comprises semicircular canals and three otolith organs (utricle, saccule, and lagena) and lacks a cochlea. The semicircular canals receive angular acceleration, as in mammals. In otolith organs, the utricle is essential for receiving linear acceleration, and the saccule and lagena are necessary for sound perception.

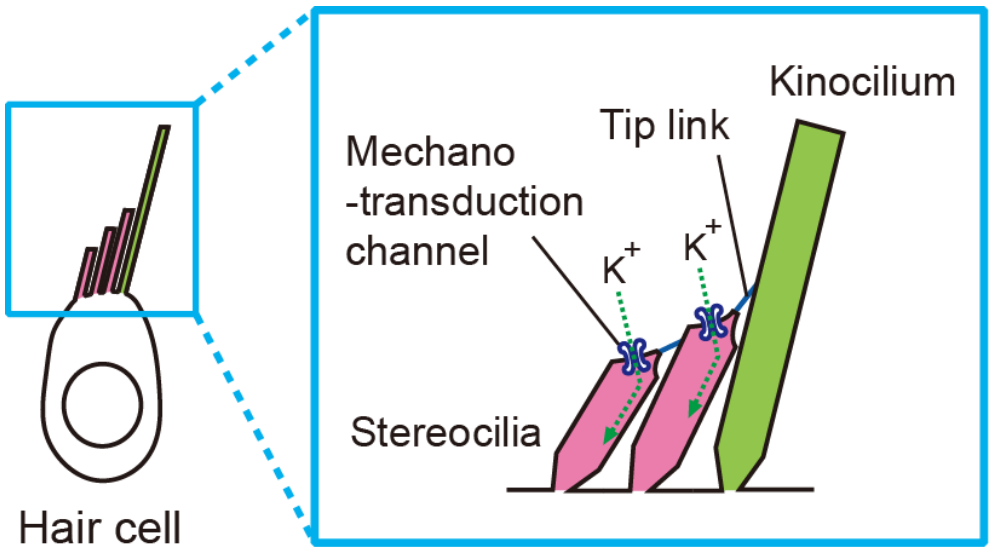

Fig. 2 Mechanotransduction machinery in hair cells

Hair bundle deflection toward the kinocilium pulls tip links between the cilia, and opens mechanotransduction channels on the tip of the stereocilia. Ion influx through the mechanotransduction channels results in depolarization of the hair cells.

Fig. 2

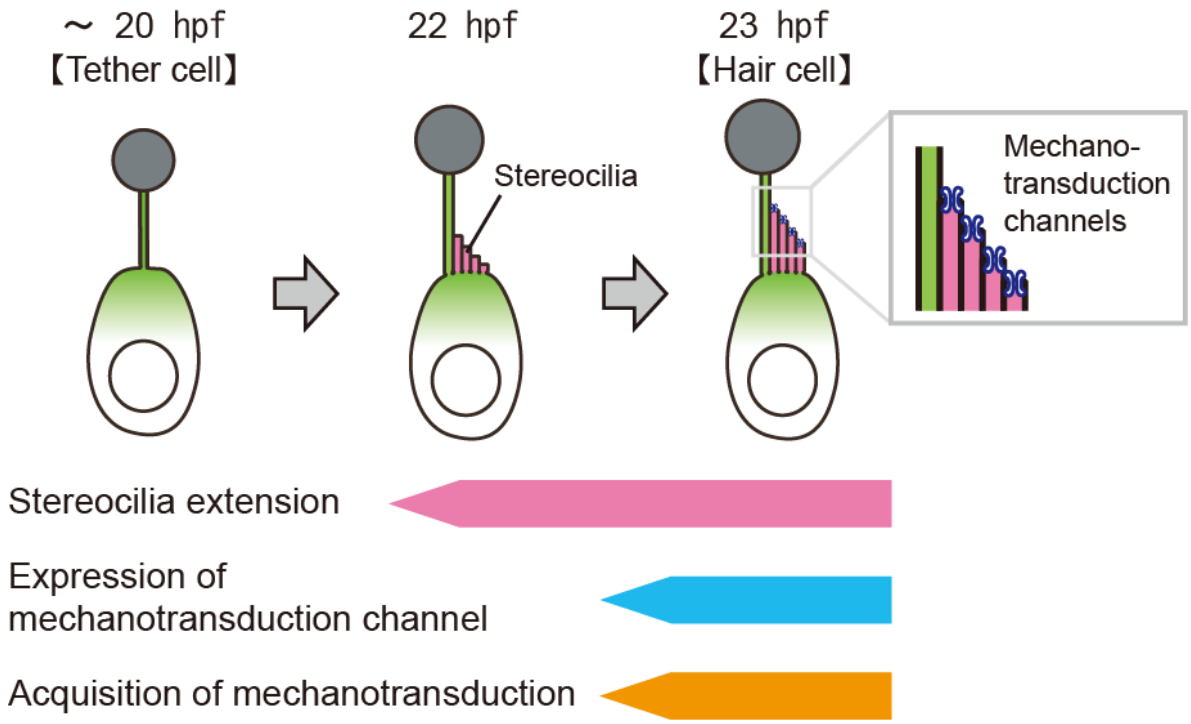

Fig. 3 Developmental acquisition of hair cell mechanotransduction in zebrafish

In the zebrafish inner ear, tether cells, which have a cilium associated with an otolith, appear by 20 hours post-fertilization (hpf). The stereocilia appears on the tether cell apex at 22 hpf and increase in ciliary length. The acquisition of mechanosensitivity is concurrent with the appearance of mechanotransduction channels in tether cells at 23 hpf.

Fig. 3

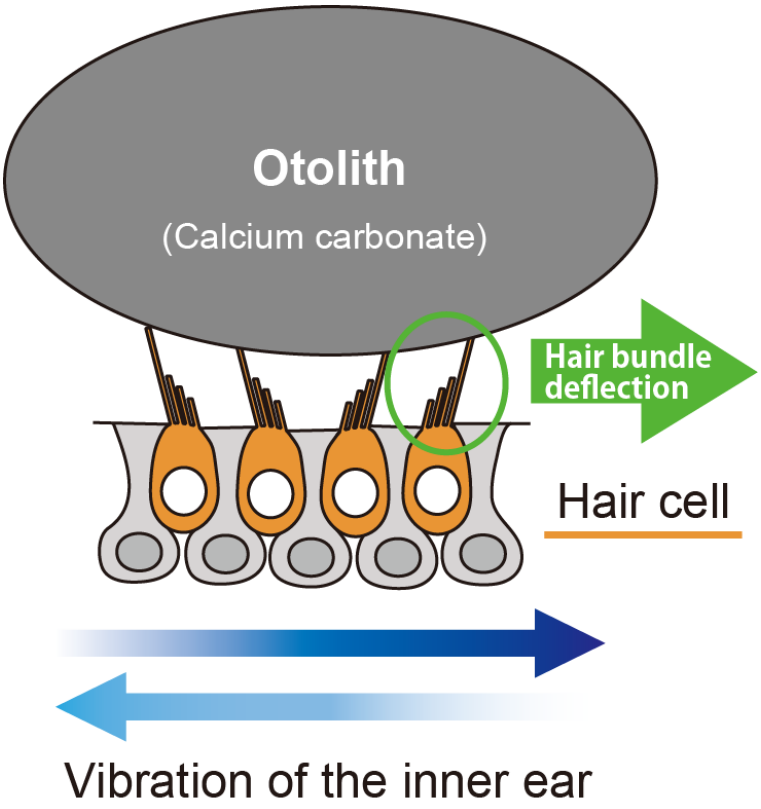

Fig. 4 Sensory reception in fish otolith organ

Otolith organs contain macular sensory hair cells coupled with an otolith, which is composed of calcium carbonate and proteins. The otolith acts as an inertial mass, and sound- and head movement-evoked acceleration produces relative displacement between the otolith and coupled hair cells because of the difference in their inertia, which causes deflection of hair bundles on the apex of hair cells.

Fig. 4

3. Results

3.1 Saccular, not utricular, hair cells transduce sound into electrical signals

Otolith organs are composed of otoliths and hair cells. For both sound and linear acceleration detection, the otolith acts as an inertial mass. Sound or linear acceleration produces relative displacement between the otolith and coupled hair cells, resulting in hair bundle deflection and the opening of the mechanotransduction channels located in the tip of hair bundles (**Hudspeth, 1989**; **Beurg et al., 2009**; **Popper and Fay, 1993, 2011**). To determine which macular hair cells detect sound, I examined the effects of the elimination of each otolith on hair cell mechanotransduction (**Figs. 5b, c**; see Materials and Methods). Opening of the mechanotransduction channels results in cation influx from the endolymph to the hair cells tip, inducing depolarization of the hair cells and negative extracellular field potentials, or MPs, around the cell bodies. MPs were recorded with a glass microelectrode inserted into OVs. A sound stimulus [90–108 dB SPL with 500 Hz; **Fig. 5h lower waveform**] elicited negative-going MPs, with peaks that were twice the frequency of the sound, as shown previously (**Fig. 5e**) (**Tanimoto et al., 2009**; **Starr et al., 2004**). When the S otolith was removed, the sound intensity range used in this study failed to evoke significant MPs (**Figs. 5g, i**), whereas MP amplitudes in the control and U otolith-removed fish increased relative to the sound intensity (**Figs. 5f, i**). These results suggest that sound was predominantly received by S hair cells in the larvae. Moreover, observation of the body postures during freely swimming indicated the

association of U otolith organs with the sense of balance. The U otolith-removed fish (n = 5) lost their balance for keeping their dorsal side up, and they showed abnormal rotation. In contrast, the S otolith-removed fish (n = 6) maintained their body posture normally.

3.2 Saccular otolith grows larger than the utricular otolith during macula-specific development

U and S are composed of otolith and hair cells and resemble each other. What key mechanisms underlie sound detection by only the S otolith organ? The developmental changes in the otolith size in each macula suggested a functional association between the otolith and sound sensitivity. I isolated the U and S otoliths from the OV at 1–5 dpf and measured their sizes. The relative otolith volumes were normalized according to the volume of the intact U otolith at 5 dpf (average of five otoliths). Both U and S otoliths noticeably grew day by day (**Fig. 6a**). At 1 dpf, the U otolith was a bit larger than the S otolith (**Figs. 6a, c**; U otolith size, 0.046 ± 0.005; S otolith size, 0.036 ± 0.003; 6 otoliths each; $P < 0.05$), as previously reported (**Riley et al., 1997**; **Murayama et al., 2005**). However, by 2 dpf, the S otolith markedly increased in size, and grew much larger than U otolith, approximately twice in size (**Figs. 6a, c**; U otolith, 0. 17 ± 0.007; S otolith, 0.33 ± 0.003; 6 otoliths each; $P < 0.001$). It was notable that the time when the size difference became apparent was concurrent with the acquisition of sound sensitivity. Sound-evoked MPs were first observed around

40 hpf in zebrafish (Tanimoto et al., 2009). The size difference became greater (Figs. 6a, c; U otolith at 3 dpf, 0. 33 ± 0.02; S otolith at 3 dpf, 0.82 ± 0.07; U otolith at 4 dpf, 0. 56 ± 0.04; S otolith at 4 dpf, 1.61 ± 0.06; 6 otoliths each; $P < 0.001$), and the S volume was approximately 2.5-fold larger than that of the U otolith at 5 dpf (Figs. 6a, c; U otolith, 1.0 ± 0.05; S otolith, 2.4 ± 0.05; 6 otoliths each; $P < 0.001$). These results suggested that the otolith size contributes to the mechanism where the S hair cells predominantly receive sound in larvae. These data also indicated that the otolith size is separately regulated in each macula during development. To confirm that otolith growth was locally regulated, I measured the size of otoliths removed from the macula. Otoliths removed from the maculae, particularly S otoliths, did not grow as large as the otoliths that remained in their normal environment (Figs. 6b, c; removed U otolith, 0.48 ± 0.02, $P < 0.001$; removed S otolith, 1.1 ± 0.08, $P < 0.001$; 6 otoliths each). This indicated that otolith growth occurred in a macular region-specific manner and differentiated the sizes of U and S otoliths.

3.3 Otolith size determines hair cell sensitivity to sound

Hair cells coupled with the massive otolith found in the S organ appear to be best suited for sensing acoustic particle motion because a larger otolith with greater inertia more effectively deflects the hair bundles (Popper and Fay, 1993, 2011). However, the association between the otolith size and sound sensitivity of hair cells was not experimentally demonstrated. I examined whether U hair cells

responded to sound stimuli when they were coupled with an enlarged otolith. To construct an enlarged U + S otolith in the U macula, I utilize the feature of fish otolith; the surface of otolith is adhesive and grows daily building a calcium carbonate layer around it (**Riley et al., 1997**; **Pannella. 1971**). I removed the S otolith and attached it to the U otolith at 1 dpf (**Fig. 7e upper right**); by 5 dpf, they had merged into one large otolith (**Figs. 5d, 7c, d, e lower right**). Sound-evoked MPs were observed in the U+S otolith fish (**Fig. 5h**). Furthermore, MP amplitudes in response to 500 Hz at 108 dB SPL were as follows: control, 237 ± 36 μV; U otolith-removed, 227 ± 30 μV; U + S otolith, 96 ± 23 μV; S otolith-removed, 20 ± 3 μV; seven fish were examined in each condition. No significant difference in MP amplitudes were observed between the control and U otolith-removed fish (P = 1.0). Amplitudes in the U + S otolith fish were smaller than those in the control or U otolith-removed fish (P = 0.043 and 0.031, respectively) but were significantly larger than those in the S otolith-removed fish (P = 0.014). These data demonstrated that U hair cells acquire sound responsiveness when coupled with a large U + S otolith. Altogether, the otolith size, at least in part, determines the hair cell sensitivity to sound.

3.4 Hair bundle polarity pattern reflects microphonic potential frequency

It is noteworthy that the MP frequency recorded from the U + S otolith fish was the same as that of the applied sound stimuli (**Fig. 5h**). This finding is in contrast with that of the biphasic response recorded from the control S macula (**Fig. 5e**). Response frequency is determined by the arrangement of the hair bundle in the macula (**Starr et al., 2004**) because mechanotransduction occurs when hair bundles deflect towards the kinocilium (**Shotwell et al., 1981**). Therefore, I labelled the hair bundles with fluorescent phalloidin to determine the association between MP frequency responses and hair bundle arrangement (**Tanimoto et al., 2011**). In the U macula, hair bundles were arranged radially from the medial edge to the lateral edge over most of the macula; at the lateral edge, a relatively small number of hair cells were oriented in the opposite direction (**Figs. 8a, b, f**). In contrast, S hair cells were classified into two anterior and two posterior groups. The two anterior groups were arranged in antiparallel patterns along the anterior-posterior axis, whereas hair bundles in the posterior two groups were arranged in a symmetrical mirror-like pattern along the dorso-ventral axis (**Figs. 8d, e, g**) (**Haddon et al., 1999**). Moreover, I found that otolith manipulation did not induce any changes in hair cell number ($P > 0.95$; **Fig. 8h**). These results confirm that monophasic MPs recorded from U + S otolith larvae were produced by U hair cells coupled with enlarged otoliths, suggesting that enlarged U + S otoliths enable U hair cells to detect acoustic particle motion. Together, these data suggest that the otolith size plays a crucial role in acoustic sensory transduction.

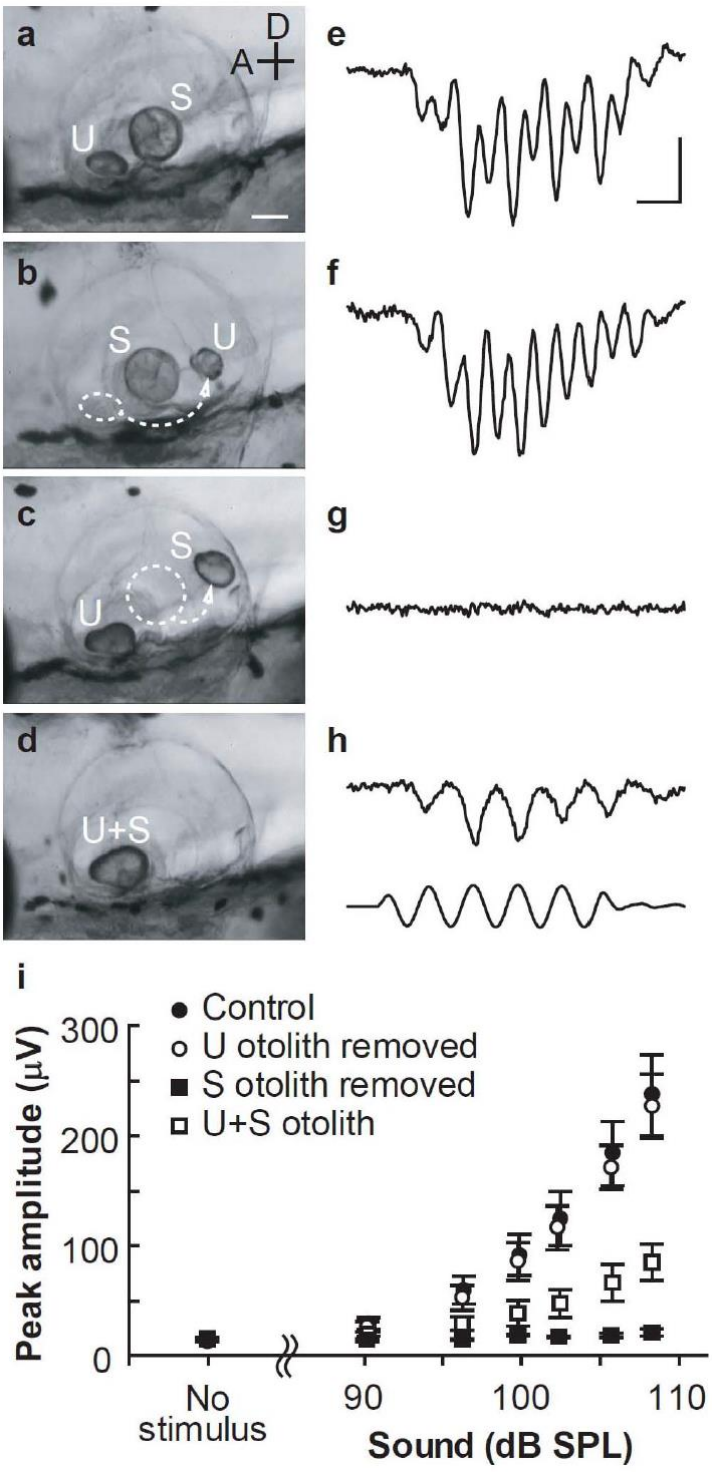
a
D
A
S
U
b
S
U
c
S
U
d
U+S
e
f
g
h
i
Control
U otolith removed
S otolith removed
U+S otolith
Peak amplitude (μV)
300
200
100
0
No stimulus
90
100
110
Sound (dB SPL)

Fig. 5

Fig. 5 The effect of otolith manipulation on sound-evoked microphonic potentials (MPs)

Lateral views of the otic vesicle (OV) (**a-d**) and MPs (**e-h**) evoked by sound stimuli [500 Hz, 5 cycles, 108 dB sound pressure level (SPL), **h** lower waveform] in control (**a, e**), utricle (U) otolith-removed (**b, f**), saccule (S) otolith-removed (**c, g**), and the utricle + saccule (U + S) otolith (**d, h**) fish. Anterior (A) and dorsal (D) axes and scale bar indicating 50 μm in (**a**) are also applicable to (**b-d**). All MP traces (**e-h**) are averages from 40 consecutive responses. Time (2 ms) and voltage (100 μV) scale bars in (**e**) are also applicable to (**f-h**). (**i**) Peak amplitudes of MPs evoked by various intensities of sound (seven fish in each condition). Error bars denote ± standard error of the mean (s.e.m.).

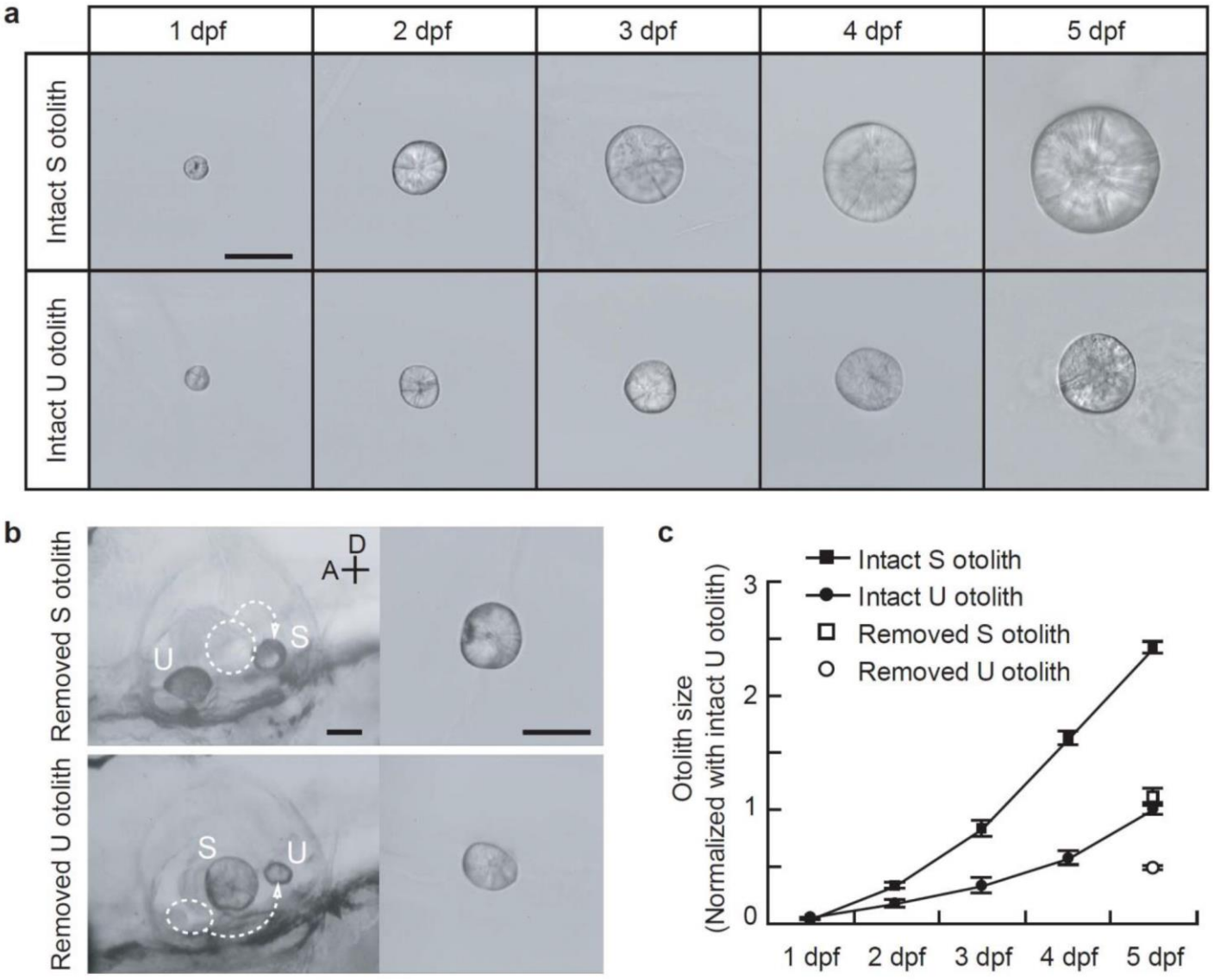
a
1 dpf
2 dpf
3 dpf
4 dpf
5 dpf
Intact S otolith
Intact U otolith
b
Removed S otolith
Removed U otolith
D
A
S
U
S
U
c
Intact S otolith
Intact U otolith
Removed S otolith
Removed U otolith
Otolith size
(Normalized with intact U otolith)
0
1
2
3
1 dpf
2 dpf
3 dpf
4 dpf
5 dpf

Fig. 6

Fig. 6 Difference in the otolith growth between saccule (S) and utricle (U) and effect of the otolith removal from its macula

(**a**) U and S otoliths isolated from intact larvae at 1–5 dpf. (**b**) Manipulated otoliths in S otolith-removed (upper panels) or U otolith-removed fish (lower panels) at 5 dpf. Left panels show lateral views of the otic vesicle (OV), and right panels show isolated otoliths. Otoliths removed from the maculae do not grow as large as normal otoliths. (**c**) Relative otolith volume normalized according to the volume of intact U otolith at 5 dpf (average of five otoliths). Scale bars represent 50 μm. Abbreviations in (**b**) indicate anterior (A) and dorsal (D). Error bars denote standard error of the mean (s.e.m.).

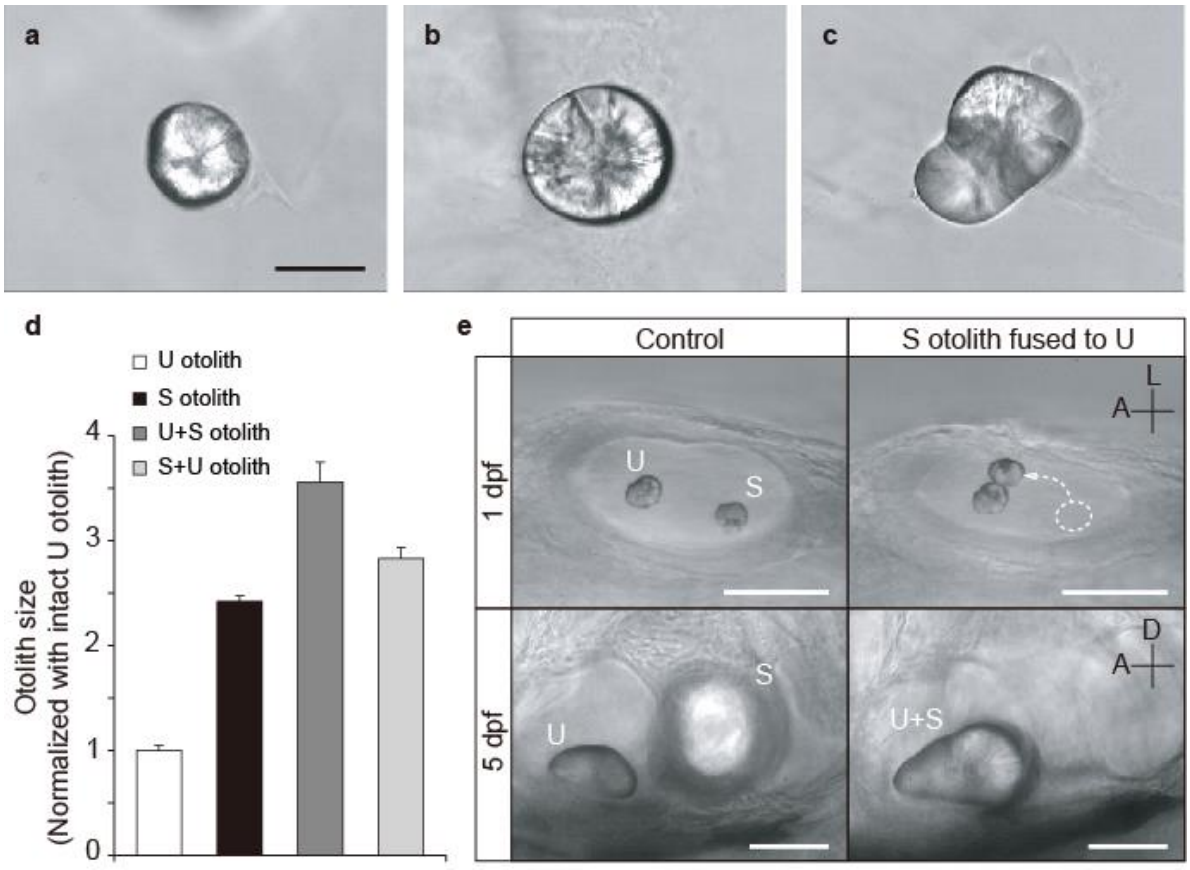
a
b
c
d
U otolith
S otolith
U+S otolith
S+U otolith
Otolith size
(Normalized with intact U otolith)
0
1
2
3
4
e
Control
S otolith fused to U
1 dpf
5 dpf
U
S
L
A
U+S
D

Fig. 7

Fig. 7 Otolith fusion results in a single large utricle + saccule (U + S) otolith

U (**a**) and S (**b**) otoliths isolated from a control larva at 5 days post-fertilization (dpf). A single U+S otolith (**c**) is produced by fusing the removed S otolith onto the U otolith at 1 dpf; fusion is confirmed at 5 dpf. (**d**) Relative otolith volume at 5 dpf normalized according to the intact U otolith volume (average of five otoliths) (see Methods). (**e**) Development of otoliths in control (left) and manipulated fish (right). Upper panels show the dorsal view of the otic vesicle (OV) at 1 dpf, and lower panels show the lateral view of OV at 5 dpf. Anterior (A) and lateral (L) axes and anterior (A) and dorsal (D) axes are applicable to (**e**) upper and lower left panels, respectively. Scale bars indicate 50 μm in all the figures. Error bars denote standard error of the mean (s.e.m.).

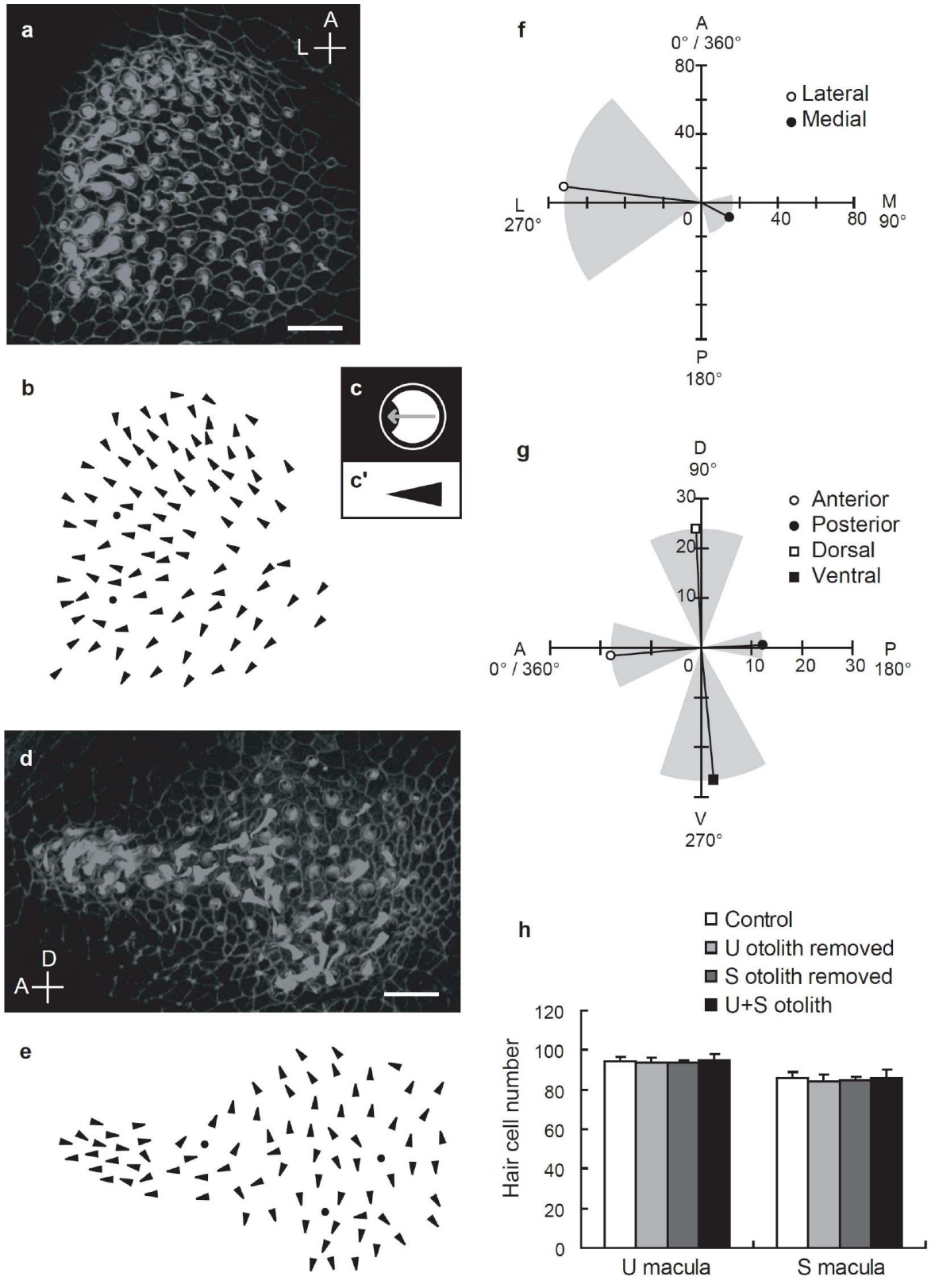
a
A
L
b
c
c'
d
D
A
e
f
A
0° / 360°
80
40
Lateral
Medial
L
270°
0
40
80
M
90°
P
180°
g
D
90°
30
20
10
Anterior
Posterior
Dorsal
Ventral
A
0° / 360°
0
10
20
30
P
180°
V
270°
h
Control
U otolith removed
S otolith removed
U+S otolith
Hair cell number
120
100
80
60
40
20
0
U macula
S macula

Fig. 8

Fig. 8 Patterns of hair bundle polarities and hair cell numbers in utricle + saccule (U+S) maculae

Stereocilia and cell boundaries are stained with fluorescent phalloidin in U (**a**) and S (**d**) maculae. Because kinocilia are not stained by phalloidin, they appear as dark spots. Hair cell polarities are determined by drawing arrowheads (**c'**) pointing from the middle of the stereociliary bundles to the middle of the kinocilium (**c**). (**b**) and (**e**) show hair bundle polarities depicted in (**a**) and (**d**), respectively. Dots indicate the positions of hair cells with unidentified polarities. (**f**, **g**) Quantification of hair bundle polarities and hair cell numbers in control S and U macula (fan-shaped areas [mean (black bars) ± standard deviation (s.d.) (gray areas)] and bar lengths, respectively) (three maculae each) (see Methods). (**h**) U and S hair cell numbers in control and manipulated-otolith maculae (5 maculae each). Scale bars indicate 10 μm (**a**, **d**). Abbreviations in (**a**, **d**, **f**, **g**) indicate anterior (A), posterior (P), lateral (L), medial (M), dorsal (D), and ventral (V). Error bars denote mean ± standard error of the mean (s.e.m.).

4. Discussion

This study demonstrated the association between sound responsiveness of hair cells and otolith, an associated extracellular structure, in the acquisition of hearing in larval zebrafish. The S otolith grew larger than the U otolith at an early developmental stage (before 5 dpf), indicating that otolith biomineralization occurred in a macular region-specific manner. The *in vivo* electrophysiological recordings of hair cell responses to sound and otolith manipulations performed to change the otolith size revealed that the otolith size was crucial for receiving auditory information in larval zebrafish.

4.1 *In vivo* recordings of hair cell mechanotransduction and otolith micromanipulation in embryonic and larval zebrafish

To achieve the extraordinary high sensitivity of hearing, the mechanotransduction machinery in hair cells and extracellular structures surrounding the hair cells are important. Therefore, analyses of isolated hair cells or slice preparations are not sufficient for investigating the mechanisms underlying sound detection in auditory organs. The present study performed *in vivo* recordings of hair cell mechanotransduction in zebrafish larvae. The simple inner ear structure and transparency of larval zebrafish (**Fig. 5a**) enabled the identification and approach to the auditory organ and the recording of the compound sound-evoked responses of the inner ear hair cells.

In addition to the transparency of the fish inner ear, the stickiness and fast growth of the fish otoliths (**Riley et al., 1997**; **Pannella 1971**) enabled the *in vivo* manipulation of changing the otolith size in zebrafish embryos (**Fig. 7**). The restricted physical manipulations in the target macula illustrated a conclusive causal relationship without the unintentional effects often occur in, for example, genetic and pharmacological analyses. Moreover, because U and S otoliths have similar compositions during development (**Riley et al., 1997**), it is improbable that the displacement of the S otolith nucleus into the U macula at 1 dpf would change the properties of U hair cells. Although it is possible that differences in the biophysical properties of the otolithic membranes or the hair cell mechanotransduction properties of hair cells may affect acoustic particle motion responsiveness, the present results indicated that the otolith size largely contributed to the differentiation of auditory and vestibular information in the fish ear. Consistent with the results of the present study, the S otolith is typically larger than the U otolith in most fish species (**Yamauchi et al., 2008**; **Bass et al., 1994**), suggesting that the fish obtained their sensitivity to sound by increasing the S otolith size.

A combination of the *in vivo* electrophysiological analyses of hair cell mechanotransduction and otolith manipulation directly demonstrated the association between the size of the extracellular structure and sound sensitivity in the auditory organ in a living animal. In addition to the otolith organs, afferent nerve pathways from the inner ear and central neural circuits are considered important in the differential transmission of auditory and vestibular information (**Popper and Fay,**

1993; Tomchik and Lu, 2005; Suwa et al., 1999). In order to distinguish linear acceleration and sound, involving tonic and phasic information, respectively, vestibular and auditory VIIIth nerves have different strategies. The vestibular VIIIth nerve encodes the magnitude of the linear acceleration in the rate of the impulse, whereas the auditory VIIIth nerve spikes during each cycle of stimulation to precisely encode the sound frequency. Therefore, it is of interest to examine how the U afferents originating from a U with an enlarged otolith transmit sound signals.

4.2 Macula-specific regulation of otolith size

The mechanisms underlying the macula-specific control of the otolith size and position are of great interest as they possibly are associated with vestibular dysfunction in humans. In this study, otoliths removed from maculae, particularly S otoliths, did not grow as large as otoliths that remained in their normal environment (Figs. 6b, c; Fig. 7) indicating that otolith growth occured in a region-specific manner. This finding was consistent with those of previous studies which showed that the components of the otolithic membrane and proteins secreted by macular hair cells and supporting cells are important for otolith development (Murayama et al., 2005; Hughes et al., 2004; Sollner et al., 2003; Lundberg et al., 2006). Further, the fusion of the U otolith to the S otolith (S + U otolith) did not result in an increase in the size of the otolith on the S macula as was the case for the U + S otolith on the U macula (Fig. 7d). This suggested that the growth of the S

otolith was strictly controlled during development so that the otolith attained a size appropriate for acoustic sensory transduction. Previous studies indicated that the genes involved in OV patterning and hair cell formation, *paired box 5* (*pax5*), *H6 family homeo box 2* and *3* (*hmx2* and *hmx3*), *fibroblast growth factor 3* (*fgf3*), are differentially expressed along the antero-posterior axis in the developing ear (**Kwak et al., 2006**; **Sapede and Pujades, 2010**; **Hammond and Whitfield, 2011**). It remains unclear if such genes and molecules contribute to macular-specific protein synthesis or the secretion processes that in turn contribute to otolith development.

4.3 Contribution of peripheral auditory structures to sound sensing in fish

Adult otophysian fish, including minnows, goldfish, and zebrafish, do not have the large S otolith. Instead, they develop Weberian ossicles that connect the inner ear to the swim bladder, which works as a sound pressure detector (**Fig. 9**; **Popper and Fay, 1993, 2011**; **Zeddies and Fay, 2005**). Weberian ossicles have not yet developed at 5 dpf, but they gradually develop to form a chain from the swim bladder to the inner ear by approximately 1 month (**Higgs et al., 2003**). Because the Weberian ossicles directly transmit the vibration of the swim bladder to the S otolith, S otoliths decrease in size and become a delicate structure during development in order to effectively receive sound-evoked vibration. The evolution of this apparatus markedly increases the sensitivity to sound pressure and also enables fish to discriminate sound frequencies.

Although fish S maculae are not equipped with basilar membranes, which are essential for the cochlea tuning in mammals, they can discriminate sound frequencies (**Jacobs and Tavolga, 1968**; **Fay, 1970**). The S macula in adult otophysian fish, which is long and narrow along the rostro-caudal axis, contains narrow otolith covered hair cells (**Platt, 1977, 1993**). In adult goldfish, S hair cells are tonotopically arranged along the rostro-caudal axis. Exposure to low-frequency sounds with a large intensity damages hair cells in the caudal the S macula, whereas the rostral hair cells are sensitive to high-frequency sounds (**Smith et al., 2011**). The measurement of S otolith movements in perch indicate that the amplitudes of vibrations vary across the length of the otolith in a frequency-dependent manner (**Sand and Michelsen, 1978**). These data indicate that the otolith play an important role in the peripheral sound frequency coding.

In contrast to adult fish, the inner ear of larva does not appear to exhibit tonotopy. In the 5-dpf zebrafish that were used in this study, the S macula was not an elongated structure (**Figs. 8d, e**; **Haddon et al., 1999**; **Platt, 1993**), and there were fewer hair cells than the adult (5-dpf larva: ~90 cells; adult: ~2,800 cells) (**Fig. 8h**; **Platt, 1993**). The otolith was shaped like an ellipsoidal hemisphere (**Fig. 7b**). These immature features were observed in both U and S maculae. Because the inner ear of larval zebrafish lacks tonotopy and *in vivo* recordings of MPs reveal the total mechanotransducer currents in the ear, the amplitude of MP is independent of the recording position.

4.4 Evolutionary associations between saccule, lagena and cochlea

Although there is apparent structural difference between the mammalian cochlea and fish S-otolith organs, the cochlea has been proposed to be an ontogenetically transformed part of the S-ototlith organ (**Fritzsch 1992**; **Fritzsch et al., 2013**). This hypothesis has been supported by the developmental expression of several genetic markers, indicating the progressive segregation of the mouse cochlea from the S during development (**Farinas et al., 2001**; **Morsli et al., 1998**). Further, several mutants, which show abnormal adjoining of the cochlea and S have been described; for example, in *Lmx1a* mutant mice, the basal half of the cochlear region shows a vestibular epithelium-like arrangement of hair cells and no tectorial membrane (**Nichols et al., 2008**). The conditional knock-out of *N-Myc* in the ear also causes fusion of the S and cochlea (**Kopecky et al., 2011**). These data suggest that segregation of the organ of Corti from S is essential for normal development and that the organ of Corti derived evolutionally from the S.

In adult fish, the lagena (L) also acts as an auditory organ (**von Frisch, 1938**). This third otolith organ is found in vertebrates ranging from fish to birds. The L develops posteriorly to the S at a much later stage of development in fish (**Bever and Fekete, 2002**). L is found on the apical part of the cochlear duct in birds, but disappears in mammals (**Harada et al., 2001**). A lack of *N-Myc* in the ear induces the transformation of the apex of the cochlea into an expanded space with a large sensory patch of hair cells (**Kopecky et al., 2011**), suggesting that the apex of the cochlea retains otolithic

organ features in part and that the L macula is integrated into the apex of the cochlea during the evolution to mammals (**Fritzsch et al., 2013**). Thus, the fish S is possibly evolutionarily differentiated into the mammalian cochlea, while the L otolith is lost.

Not only the sensory epithelia, but also the extracellular structures covering the hair cells share their origin. The tectorial membrane and otolith express numerous common proteins (**Goodyear and Richardson, 2002**). Furthermore, it is suggested that the absence of Wnt signaling induces transformation from an otolith organ to the cochlea in evolutionary and ontogenetic processes (**Stevens et al., 2003**). Overexpression of an activated form of β-catenin that should constitutively activate the Wnt signaling pathway during an early critical phase of otic development converts the extracellular structure from a tectorial membrane to an otolith-based structure in chicks. Moreover *Wnt3a* misexpression results in the production of ectopic vestibular patches in the cochlear duct.

The results of this study indicated that otolith development is a critical step in the acquisition of hearing in larval zebrafish. These findings were consistent with anatomical observations in rodents that suggest the requirement of a developed tectorial membrane for hearing onset (**Roth and Bruns, 1992**; **Rueda et al., 1996**; **Kopecky et al., 2012**). Thus, although the fish S is much simpler auditory organ than the mammalian cochlea, it has a common origin and similar processes underlie the acquisition of hearing. This analysis of the acquisition of auditory responses in fish otolith organs provided new insights into how vertebrates develop the sense of sound.

4.5 Concluding remarks

Anatomical defects in the extracellular structures of inner ear hair cells cause clinical disorders, wherein patients have difficulty in separating acoustic stimuli from vestibular signals. Patients suffering from superior canal dehiscence syndrome or enlarged vestibular aqueduct syndrome show abnormal activation of vestibular reflexes in response to sound (**Minor et al., 1998**; **Valvassori and Clemis, 1978**). To investigate the neuronal mechanisms underlying these sensory separation problems, a better understanding of the evolutionary transformation of the auditory organ from the vestibular organ is required (**Carey and Amin, 2006**).

The mechanisms underlying the proper formation of extracellular structures and the separation of auditory and vestibular perception are important for understanding the development of different senses. In addition to the findings of this study, *in vivo* live imaging have visualized otolith formation in embryonic and larval zebrafish (**Colantonio et al., 2009; Wu et al., 2011**; **Stooke-Vaughan et al., 2012**). Furthermore, various genes required for otolith formation have been identified (**Murayama et al., 2005**; **Hughes et al., 2004**; **Sollner et al., 2003**; **Lundberg et al., 2006**). Advances in molecular genetic techniques, morphological observations, and electrophysiological recordings in zebrafish *in vivo* enable us to study the function and morphogenesis of otoliths and pave the way for a better understanding of the functional acquisition of acoustic and vestibular sensory transduction in the inner ear.

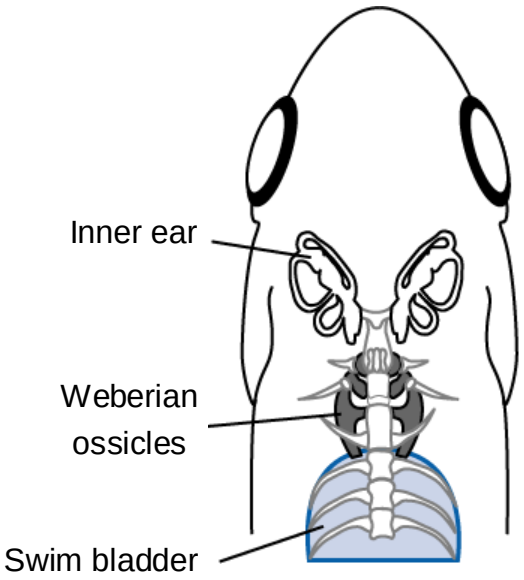

Fig. 9 Detection of sound pressure in adult Ostariophysi (bony fish)

When the outside sound pressure is increased, the volume of the swim bladder should be reduced. This results a pull on the Weberian ossicles. The movements are transmitted to the saccule where they cause a dorsal-ward movement of the saccular otolith. In contrast, a decrease in the outside pressure produces a ventral-ward movement of the otolith (After **von Frisch, 1938**).

Fig. 9

5. Materials and Methods

Animals

Adult wild-type zebrafish (*Danio rerio*) obtained from a local supplier (Meito Suien, Japan) were maintained as a breeding colony. Embryos and larvae were reared at 28.5°C and staged according to standard procedures (**Kimmel et al., 1995**). The experiments described below were performed at 26 to 28°C. All procedures complied with the guidelines stipulated by the Nagoya University Committee on Animal Research.

Electrophysiological recordings of microphonic potentials

Larvae at 5 dpf were temporarily anesthetized in 0.02% tricaine methanesulfonate (MS-222; Sigma-Aldrich) and then immobilized in 1 mM d-tubocurarine (Sigma-Aldrich) for approximately 10 min. The larvae were securely attached with tungsten pins on a Sylgard-coated glass-bottomed dish filled with extracellular solution containing (in mM) 134 NaCl, 2.9 KCl, 1.2 $MgCl_2$, 2.1 $CaCl_2$, 10 HEPES, and 10 glucose, at 290 mOsm, adjusted to pH 7.8 with NaOH. The dish was attached to a recording stage (ITS-02, Narishige), using double-sided sticky tape and observed through a 40× water-immersion objective lens (LUMPLFL 40XW, Olympus) equipped on an upright microscope (BX51WI, Olympus). Sinusoidal waveforms for sound stimulation (500 Hz, 5 cycles) were generated by a function generator (Wave Factory 1941, NF Electronic Instruments), amplified by an

audio amplifier (PMA-390, Denon), and transmitted into the air through a loudspeaker (101SDVM, Bose) positioned 45 cm lateral to the fish. SPLs were measured using a sound level meter (LA-215, Ono Sokki). Recording micropipettes were made from borosilicate glass capillaries (GD-1.5, Narishige) using a pipette puller (P-97, Sutter Instrument). An MP recording micropipette filled with the abovementioned extracellular solution (resistance, 5–10 MΩ) was inserted into the OV by using a micromanipulator (MPC-200, Sutter Instrument Co.) and was held with a stiff glass rod to reduce vibration during exposure to the applied sound stimuli. MPs were sampled at 20 kHz using a MultiClamp 700B amplifier (Molecular Devices) and Clampex 10.2 software (Molecular Devices), and were analysed using Clampfit 10.2 software (Molecular Devices).

Otolith manipulation

Embryos were manually removed from chorions and anesthetized in 0.02% tricaine methanesulfonate for approximately 3 min, and were subsequently held in a Sylgard-coated glass-bottomed dish filled with the abovementioned extracellular solution. A micropipette was inserted into the OV as described above, and the U or S otolith was selectively removed from the macula at 2 dpf. To construct the fused large U + S otolith in the U macula, the S otolith was removed from its macula and positioned adjacent to the U otolith at 1 dpf. Embryos with manipulated otoliths were reared to 5 dpf for further electrophysiological and morphological

experiments.

Otolith size measurement

Otolith size was measured as described previously (**Lychakov and Rebane, 2000**) with some modifications. Briefly, 5 dpf larvae were anaesthetised in 0.02% tricaine methanesulfonate and embedded in 5% agar, and otoliths were removed from the OVs using a fine tungsten pin. The otoliths were embedded in 5% agar with the macular surface facing downwards. The top-view images (**Figs. 6, 7a-c**) were captured by a charge-coupled device camera (C2741-79H; Hamamatsu Photonics) mounted on a microscope (BX51WI; Olympus). The otolith was then rotated by 90 degrees, and lateral-view images were captured. The base area and height of the otolith were measured in the captured images using Photoshop 7.0.1 (Adobe). The products of the base area and height were normalized to that of an intact U otolith to calculate the relative volume for each otolith.

Phalloidin staining and confocal imaging

Five dpf larvae were immunostained as described previously (**Tanimoto et al., 2011**; **Haddon et al., 1999**). Larvae were fixed in 4% paraformaldehyde in 0.1 M phosphate-buffered solution (PBS) at 4°C overnight. After permeabilization of the samples with acetone for 10 min at –20°C, hair cell stereocilia were visualized with 1:100 dilution of Alexa Fluor 568 phalloidin (A12380; Invitrogen)

in 0.1 M PBS containing 2% Triton X-100.

Coronal and sagittal cryosections of 60 μm thickness were obtained to observe the U and S, respectively. The sections were observed through a 100× oil immersion objective lens on a microscope (BX50WI, Olympus). The fluorescent images were captured at 0.5 μm z-axis intervals using a confocal laser scanning system (FV300; Olympus) and data acquisition software (Fluoview; Olympus).

Analysis of hair bundle polarity

The hair bundle polarity was determined by drawing arrowheads pointing from the middle of the phalloidin-stained stereocilia to the kinocilia, which appeared as dark spots (**Figs. 8c and c′**) (**Tanimoto et al., 2011**; **Haddon et al., 1999**). To quantify hair bundle arrangement in U, we defined the anterior side as 0°/360°; therefore, the medial, posterior, and lateral directions were expressed as 90°, 180°, and 270°, respectively (in the coronal section, **Fig. 8f**). Hair cells with hair bundles oriented between 0° and 180° were classified into the medial direction group, and those oriented between 180° and 360° into the lateral direction group (**Fig. 8f**). Similarly, the anterior side was defined as 0°/360° in S; therefore, the dorsal, posterior, and ventral directions were expressed as 90°, 180°, and 270°, respectively (in the sagittal section, **Fig. 8g**). S hair cells were divided into four groups according to the orientations of their hair bundles: anterior (0°–45° or 315°–360°), dorsal

(45°–135°), posterior (135°–225°), and ventral (225°–315°) (**Fig. 8g**).

Statistics

All values were expressed as mean ± standard error of the mean with the exception of those in **Figs. 8f and g**, where the values were expressed as standard deviations. MP amplitudes were statistically analysed using the Steel–Dwass test for nonparametric multiple comparisons. The same results were obtained by the Mann–Whitney test with Bonferroni correction. The number of hair cells was statistically analysed using the Dunnett's test for comparison with control maculae.

6. References

Abbas, L., Whitfield, T. T., Perry, S., Ekker, M., Farrell, A., & Brauner, C. The zebrafish inner ear. *Fish Physiology: Zebrafish: Zebrafish* **29**, 123 (2010).

Bass, A. H., Marchaterre, M. A. & Baker, R. Vocal-acoustic pathways in a teleost fish. *The Journal of neuroscience* **14**, 4025-4039 (1994).

Baylor, D. A., Lamb, T. D. & Yau, K. W. Responses of retinal rods to single photons. *The Journal of physiology* **288**, 613-634 (1979).

Beck, J. C., Gilland, E., Tank, D. W. & Baker, R. Quantifying the ontogeny of optokinetic and vestibuloocular behaviors in zebrafish, medaka, and goldfish. *Journal of neurophysiology* **92**, 3546-3561 (2004).

Beurg, M., Fettiplace, R., Nam, J. H. & Ricci, A. J. Localization of inner hair cell mechanotransducer channels using high-speed calcium imaging. *Nature neuroscience* **12**, 553-558 (2009).

Bever, M. M. & Fekete, D. M. Atlas of the developing inner ear in zebrafish. *Developmental dynamics* **223**, 536-543 (2002).

Bianco, I. H., Ma, L.H., Schoppik, D., Robson, D.N., Orger, M.B., Beck, J.C., Li, J.M., Schier, A.F., Engert, F., & Baker, R. The tangential nucleus controls a gravito-inertial vestibulo-ocular reflex. *Current biology* **22**, 1285-1295 (2012).

Blatchley, B. J., Cooper, W. A. & Coleman, J. R. Development of auditory brainstem response to tone pip stimuli in the rat. *Brain research* **429**, 75-84 (1987).

Carey, J. & Amin, N. Evolutionary changes in the cochlea and labyrinth: Solving the problem of sound transmission to the balance organs of the inner ear. *The anatomical record.* **288**, 482-489 (2006).

Colantonio, J. R. Vermot, J., Wu, D., Langenbacher, A.D., Fraser, S., Chen, J.N., & Hill, K.L. The dynein regulatory complex is required for ciliary motility and otolith biogenesis in the inner ear. *Nature* **457**, 205-209 (2009).

Denman-Johnson, K. & Forge, A. Establishment of hair bundle polarity and orientation in the developing vestibular system of the mouse. *Journal of neurocytology* **28**, 821-835 (1999).

Farinas, I., Jones, K.R., Tessarollo, L., Vigers, A.J., Huang, E., Kirstein, M., de Caprona, D.C., Coppola, V., Backus, C., Reichardt, L.F., *et al.* Spatial shaping of cochlear innervation by temporally regulated neurotrophin expression. *The Journal of neuroscience* **21**, 6170-6180 (2001).

Fay, R. R. Auditory frequency generalization in the goldfish (Carassius auratus). *Journal of the experimental analysis of behavior* **14**, 353-360 (1970).

Fritzsch, B. The water-to-land transition: evolution of the tetrapod basilar papilla, middle ear, and auditory nuclei. *The evolutionary biology of hearing (Springer)*, 351-375. (1992).

Fritzsch, B., Pan, N., Jahan, I., Duncan, J.S., Kopecky, B. J., Elliott, K.L., Kersigo, J., and Yang, T. Evolution and development of the tetrapod auditory system: an organ of Corti-centric perspective. *Evolution & development* **15**, 63-79 (2013).

Geal-Dor, M., Freeman, S., Li, G. & Sohmer, H. Development of hearing in neonatal rats: air and bone conducted ABR thresholds. *Hearing research* **69**, 236-242 (1993).

Geleoc, G. S. & Holt, J. R. Developmental acquisition of sensory transduction in hair cells of the mouse inner ear. *Nature neuroscience* **6**, 1019-1020 (2003).

Goodyear, R. J. & Richardson, G. P. Extracellular matrices associated with the apical surfaces of sensory epithelia in the inner ear: molecular and structural diversity. *Journal of neurobiology* **53**, 212-227 (2002).

Haddon, C. & Lewis, J. Early ear development in the embryo of the zebrafish, Danio rerio. *The Journal of comparative neurology* **365**, 113-128 (1996).

Haddon, C., Mowbray, C., Whitfield, T., Jones, D., Gschmeissner, S., and Lewis, J. Hair cells without supporting cells: further studies in the ear of the zebrafish mind bomb mutant. *Journal of neurocytology* **28**, 837-850 (1999).

Hammond, K. L. & Whitfield, T. T. Fgf and Hh signalling act on a symmetrical pre-pattern to specify anterior and posterior identity in the zebrafish otic placode and vesicle. *Development* **138**, 3977-3987 (2011).

Harada, Y., Kasuga, S. & Tamura, S. Comparison and evolution of the lagena in various animal species. *Acta oto-laryngologica* **121**, 355-363 (2001).

Higgs, D. M., Rollo, A. K., Souza, M. J. & Popper, A. N. Development of form and function in peripheral auditory structures of the zebrafish (Danio rerio). *The Journal of the Acoustical Society of America* **113**, 1145-1154 (2003).

Hudspeth, A. J. How the ear's works work. *Nature* **341**, 397-404 (1989).

Hughes, I., Blasiole, B., Huss, D., Warchol, M.E., Rath, N.P., Hurle, B., Ignatova, E., Dickman, J.D., Thalmann, R., Levenson, R., *et al.* Otopetrin 1 is required for otolith formation in the zebrafish Danio rerio. *Developmental biology* **276**, 391-402 (2004).

Jacobs, D. W. & Tavolga, W. N. Acoustic frequency discrimination in the goldfish. *Animal behaviour* **16**, 67-71 (1968).

Johansson, R. S. Tactile sensibility in the human hand: receptive field characteristics of mechanoreceptive units in the glabrous skin area. *The Journal of physiology* **281**, 101-125 (1978).

Kazmierczak, P., Sakaguchi, H., Tokita, J., Wilson-Kubalek, E.M., Milligan, R.A., Muller, U., & Kachar, B. Cadherin 23 and protocadherin 15 interact to form tip-link filaments in sensory hair cells. *Nature* **449**, 87-91 (2007).

Kenshalo, D. R., Nafe, J. P., & Dawson, W. W. A new method for the investigation of thermal sensitivity. *The Journal of psychology* **49** (1), 29-41 (1960)

Kimmel, C. B., Ballard, W. W., Kimmel, S. R., Ullmann, B. & Schilling, T. F. Stages of embryonic development of the zebrafish. *Developmental dynamics* **203**, 253-310, (1995).

Kimmel, C. B., Patterson, J. & Kimmel, R. O. The development and behavioral characteristics of the startle response in the zebra fish. *Developmental psychobiology* **7**, 47-60 (1974).

Kopecky, B., Johnson, S., Schmitz, H., Santi, P. & Fritzsch, B. Scanning thin-sheet laser imaging microscopy elucidates details on mouse ear development. *Developmental dynamics* **241**, 465-480 (2012).

Kopecky, B., Santi, P., Johnson, S., Schmitz, H. & Fritzsch, B. Conditional deletion of N-Myc disrupts neurosensory and non-sensory development of the ear. *Developmental dynamics* **240**, 1373-1390 (2011).

Kwak, S. J. Vemaraju, S., Moorman, S.J., Zeddies, D., Popper, A.N., & Riley, B.B. Zebrafish pax5 regulates development of the utricular macula and vestibular function. *Developmental dynamics* **235**, 3026-3038 (2006).

Legan, P. K., Vemaraju, S., Moorman, S.J., Zeddies, D., Popper, A.N., & Riley, B.B. A deafness mutation isolates a second role for the tectorial membrane in hearing. *Nature neuroscience* **8**, 1035-1042 (2005).

Lelli, A., Asai, Y., Forge, A., Holt, J. R. & Geleoc, G. S. Tonotopic gradient in the developmental acquisition of sensory transduction in outer hair cells of the mouse cochlea. *Journal of neurophysiology* **101**, 2961-2973 (2009).

Lelli, A., Kazmierczak, P., Kawashima, Y., Muller, U. & Holt, J. R. Development and regeneration of sensory transduction in auditory hair cells requires functional interaction between cadherin-23 and protocadherin-15. *The Journal of neuroscience* **30**, 11259-11269 (2010).

Lenoir, M., Shnerson, A. & Pujol, R. Cochlear receptor development in the rat with emphasis on synaptogenesis. *Anatomy and embryology* **160**, 253-262 (1980).

Limb, C. J. & Ryugo, D. K. Development of primary axosomatic endings in the anteroventral cochlear nucleus of mice. *Journal of the Association for Research in Otolaryngology* **1**, 103-119 (2000).

Lundberg, Y. W., Zhao, X. & Yamoah, E. N. Assembly of the otoconia complex to the macular sensory epithelium of the vestibule. *Brain research* **1091**, 47-57 (2006).

Lychakov, D. V. & Rebane, Y. T. Otolith regularities. *Hearing research* **143**, 83-102 (2000).

Minor, L. B., Solomon, D., Zinreich, J. S. & Zee, D. S. Sound-and/or pressure-induced vertigo due to bone dehiscence of the superior semicircular canal. *Archives of Otolaryngology–Head & Neck Surgery* **124**, 249-258 (1998).

Morsli, H., Choo, D., Ryan, A., Johnson, R. & Wu, D. K. Development of the mouse inner ear and origin of its sensory organs. *The Journal of neuroscience* **18**, 3327-3335 (1998).

Murayama, E., Herbomel, P., Kawakami, A., Takeda, H. & Nagasawa, H. Otolith matrix proteins OMP-1 and Otolin-1 are necessary for normal otolith growth and their correct anchoring onto the sensory maculae. *Mechanisms of development* **122**, 791-803 (2005).

Neises, G. R., Mattox, D. E. & Gulley, R. L. The maturation of the end bulb of Held in the rat anteroventral cochlear nucleus. *The Anatomical record* **204**, 271-279 (1982).

Nichols, D. H. Santi, P., Johnson, S., Schmitz, H., and Fritzsch, B. Lmx1a is required for segregation of sensory epithelia and normal ear histogenesis and morphogenesis. *Cell and tissue research* **334**, 339-358 (2008).

Panella, G. Fish otoliths: daily growth layers and periodical patterns. *Science* **173**, 1124-1127 (1971).

Platt, C. Hair cell distribution and orientation in goldfish otolith organs. *The Journal of comparative neurology* **172**, 283-287 (1977).

Platt, C. Zebrafish inner ear sensory surfaces are similar to those in goldfish. *Hearing research* **65**, 133-140 (1993).

Popper, A. N. & Fay, R. R. Sound detection and processing by fish: critical review and major research questions. *Brain, behavior and evolution* **41**, 14-38 (1993).

Popper, A. N. & Fay, R. R. Rethinking sound detection by fishes. *Hearing research* **273**, 25-36 (2011).

Riley, B. B. & Moorman, S. J. Development of utricular otoliths, but not saccular otoliths, is necessary for vestibular function and survival in zebrafish. *Journal of neurobiology* **43**, 329-337 (2000).

Riley, B. B., Zhu, C., Janetopoulos, C. & Aufderheide, K. J. A critical period of ear development controlled by distinct populations of ciliated cells in the zebrafish. *Developmental biology* **191**, 191-201 (1997).

Roth, B. & Bruns, V. Postnatal development of the rat organ of Corti. I. General morphology, basilar membrane, tectorial membrane and border cells. *Anatomy and embryology* **185**, 559-569 (1992).

Rueda, J., Cantos, R. & Lim, D. J. Tectorial membrane-organ of Corti relationship during cochlear development. *Anatomy and embryology* **194**, 501-514 (1996).

Russell, I. J., Legan, P. K., Lukashkina, V. A., Lukashkin, A. N., Goodyear, R. J., & Richardson, G. P. Sharpened cochlear tuning in a mouse with a genetically modified tectorial membrane. *Nature neuroscience* **10**, 215-223 (2007).

Sand, O. & Michelsen, A. Vibration measurements of the perch saccular otolith. *Journal of comparative physiology* **123**, 85-89 (1978).

Sapede, D. & Pujades, C. Hedgehog signaling governs the development of otic sensory epithelium and its associated innervation in zebrafish. *The Journal of neuroscience* **30**, 3612-3623 (2010).

Seiler, C., Finger-Baier, K.C., Rinner, O., Makhankov, Y.V., Schwarz, H., Neuhauss, S.C., & Nicolson, T. Duplicated genes with split functions: independent roles of protocadherin15 orthologues in zebrafish hearing and vision. *Development* **132**, 615-623 (2005).

Shotwell, S. L., Jacobs, R. & Hudspeth, A. J. Directional sensitivity of individual vertebrate hair cells to controlled deflection of their hair bundles. *Annals of the New York Academy of Sciences* **374**, 1-10 (1981).

Si, F., Brodie, H., Gillespie, P. G., Vazquez, A. E. & Yamoah, E. N. Developmental assembly of transduction apparatus in chick basilar papilla. *The Journal of neuroscience* **23**, 10815-10826 (2003).

Smith, M. E., Schuck, J. B., Gilley, R. R. & Rogers, B. D. Structural and functional effects of acoustic exposure in goldfish: evidence for tonotopy in the teleost saccule. *BMC neuroscience* **12**, 19 (2011).

Sobkowicz, H. M., Rose, J. E., Scott, G. E. & Slapnick, S. M. Ribbon synapses in the developing intact and cultured organ of Corti in the mouse. *The Journal of neuroscience* **2**, 942-957 (1982).

Sollner, C., Burghammer, M., Busch-Nentwich, E., Berger, J., Schwarz, H., Riekel, C., & Nicolson, T. Control of crystal size and lattice formation by starmaker in otolith biomineralization. *Science* **302**, 282-286 (2003).

Sollner, C., Rauch, G. J., Siemens, J., Geisler, R., Schuster, S. C., Muller, U., Nicolson, T., & Tubingen Screen, C. Mutations in cadherin 23 affect tip links in zebrafish sensory hair cells. *Nature* **428**, 955-959 (2004).

Starr, C. J., Kappler, J. A., Chan, D. K., Kollmar, R. & Hudspeth, A. J. Mutation of the zebrafish choroideremia gene encoding Rab escort protein 1 devastates hair cells. *Proceedings of the National Academy of Sciences of the United States of America* **101**, 2572-2577 (2004).

Stevens, C. B., Davies, A. L., Battista, S., Lewis, J. H. & Fekete, D. M. Forced activation of Wnt signaling alters morphogenesis and sensory organ identity in the chicken inner ear. *Developmental biology* **261**, 149-164 (2003).

Stooke-Vaughan, G. A., Huang, P., Hammond, K. L., Schier, A. F. & Whitfield, T. T. The role of hair cells, cilia and ciliary motility in otolith formation in the zebrafish otic vesicle. *Development* **139**, 1777-1787 (2012).

Suwa, H., Gilland, E. & Baker, R. Otolith ocular reflex function of the tangential nucleus in teleost fish. *Annals of the New York Academy of Sciences* **871**, 1-14 (1999).

Tanimoto, M., Ota, Y., Horikawa, K. & Oda, Y. Auditory input to CNS is acquired coincidentally with development of inner ear after formation of functional afferent pathway in zebrafish. *The Journal of neuroscience* **29**, 2762-2767 (2009).

Tanimoto, M., Ota, Y., Inoue, M. & Oda, Y. Origin of inner ear hair cells: morphological and functional differentiation from ciliary cells into hair cells in zebrafish inner ear. *The Journal of neuroscience* **31**, 3784-3794 (2011).

Tomchik, S. M. & Lu, Z. Octavolateral projections and organization in the medulla of a teleost fish, the sleeper goby (Dormitator latifrons). *The Journal of comparative neurology* **481**, 96-117 (2005).

Valvassori, G. & Clemis, J. The large vestibular aqueduct syndrome. *The Laryngoscope* **88**, 723-728 (1978).

von Frisch, K. The sense of hearing in fish. *Nature* **141**, 8-11 (1938).

Waguespack, J., Salles, F. T., Kachar, B. & Ricci, A. J. Stepwise morphological and functional maturation of mechanotransduction in rat outer hair cells. *The Journal of neuroscience* **27**, 13890-13902 (2007).

Wheeler, L. J. & Dickson, E. D. The determination of the threshold of hearing. *The Journal of laryngology and otology* **66**, 379-395 (1952).

Whitfield, T. T., Riley, B. B., Chiang, M. Y. & Phillips, B. Development of the zebrafish inner ear. *Developmental dynamics* **223**, 427-458 (2002).

Wu, D., Freund, J. B., Fraser, S. E. & Vermot, J. Mechanistic basis of otolith formation during teleost inner ear development. *Developmental cell* **20**, 271-278 (2011).

Yamauchi, M., Tanaka, J. & Harada, Y. Comparative study on the morphology and the composition of the otoliths in the teleosts. *Acta oto-laryngologica* **128**, 846-855 (2008).

Zeddies, D. G. & Fay, R. R. Development of the acoustically evoked behavioral response in zebrafish to pure tones. *The Journal of experimental biology* **208**, 1363-1372 (2005).

7. Acknowledgments

I would like to express my deepest gratitude to Dr. Yoichi Oda for his kind instruction, helpful discussion, critical comments, and consistent encouragement since I joined the laboratory of Brain Function and Structure. I also greatly appreciate Dr. Masashi Tanimoto for his helpful instruction for the experiments and discussion of my work as a collaborator. I would also like to express my appreciation to Drs. Shin Takagi and Hiroko Bannai for providing important comments. I thank all the laboratory members and staff for their helpful discussions and encouragement. I am also grateful to Dr. Azusa Kamikouchi for kindly proofreading my doctoral thesis.

This work was supported by a Grant-in-Aid for Scientific Research (KAKENHI; 22300126, 23115508 and 25127705), a Grant-in-Aid for the Japan Society for the Promotion of Science (JSPS) Fellows, the Uehara Memorial Foundation, the Hori Sciences and Arts Foundation, and the Ichihara International Scholarship Foundation.

副論文

The role of ear stone size in hair cell acoustic sensory transduction

(有毛細胞での音信号から感覚情報への信号変換における耳石の役割)

Maya Inoue, Masashi Tanimoto, & Yoichi Oda

Scientific Reports **3**, 2114 (2013)

参考論文

Origin of Inner Ear Hair Cells: Morphological and Functional Differentiation from Ciliary Cells into Hair Cells in Zebrafish Inner Ear

(内耳有毛細胞の起源：ゼブラフィッシュ内耳における繊毛性細胞の有毛細胞への形態学的・機能的な分化)

Masashi Tanimoto, Yukiko Ota, Maya Inoue & Yoichi Oda

The Journal of neuroscience **31**, 3784-3794 (2011)